Departement für Pferde, Klinik für Pferdechirurgie
der Vetsuisse-Fakultät Universität Zürich

Direktor: Prof. Dr. med. vet. Anton Fürst, Dipl. ECVS

Arbeit unter der wissenschaftlichen Betreuung von
Dr. med. vet. Andrea Bischofberger, Dipl. ACVS/ECVS

Validation of delayed gadolinium – enhanced magnetic resonance imaging of cartilage and T2 mapping for quantifying distal interphalangeal joint cartilage thickness in Warmblood horses

Inaugural-Dissertation

zur Erlangung der Doktorwürde der
Vetsuisse-Fakultät Universität Zürich

vorgelegt von

Regula Fürst

Tierärztin
von Dietikon

genehmigt auf Antrag von

Prof. Dr. med. vet. Anton Fürst, Dipl. ECVS, Referent
Prof. Dr. med. vet. Patrick Robert Kircher, PhD, Dipl. ECVDI, Korreferent

2017

Meinen Eltern Max und Marlies Fürst,
welche mich immer grosszügig unterstützen

Inhaltsverzeichnis

1 Summary

The objective of this study was to determine whether delayed – gadolinium enhanced magnetic resonance imaging of the cartilage (dGEMRIC) and T2 mapping are accurate techniques for measuring cartilage thickness in the distal interphalangeal joint (DIPJ) of Warmblood horses.

Twelve cadaver forelimbs were acquired from twelve Warmblood horses with a mean age of 15 (6 – 32) years showing no signs of lameness. Cartilage thickness was measured from dGEMRIC images as well as in T2 maps in 9 regions of interest (ROIs) in the distal cartilage of the middle phalanx (P2) and in 9 ROIs in the proximal cartilage of the distal phalanx (P3). The measurements from the MRI were compared with the cartilage thicknesses measured in the corresponding histological images. Histological cartilage thicknesses were measured at 11 ROIs on P2 and P3. The histological sections of the different ROIs were graded on the basis of the Mankin scoring system and the ROIs classified into three groups of cartilage health.

This study found that the histological cartilage thickness measurements significantly correlated with the dGEMRIC (T1) and T2 cartilage thickness measurements. The measurements did not differ significantly from the dGEMRIC (T1) and T2 cartilage thickness measurements. The correlation between the T1 measurements and the histological measurements were always better than the T2 measurements compared to the histological measurements.

The T1, T2 as well as the histological measurements showed that the joint disease state has a significant effect on the cartilage thickness measurements. As expected increasing degree of osteoarthritis lead to a decreasing cartilage thickness. Normal cartilage was significantly thicker than mildly – moderate diseased cartilage, and mildly – moderate diseased cartilage was also significantly thicker than severely diseased cartilage.

There were regional differences in cartilage thickness depending on the cartilage site within the joint. So, the cartilage of P2 is thinner than the P3 cartilage and the central

areas are larger than the palmar zones. Finally is the condylar cartilage thinner than the intercondylar one.
The joint space width (JSW), measured at 9 locations within the DIPJ, is generally smaller when measured on T2 maps than on T1 maps. The JSW correlations of the mean T1 measurements with the histological measurements (total and hyaline cartilage) were stronger than the correlations of the T2 measurements with the histological measurements.

Based on these results, the normal or degenerated equine articular cartilage can be evaluated by dGEMRIC or T2 maps at areas of opposing or non-opposing cartilage surfaces. In doing so, the T1 measurements are more suitable than the T2 ones.

2 Manuscript

2.1 Introduction

The main reason for weak performance and wastage in horses is lameness.(1) In North America the decrease in athletic ability has been estimated to cost the performance horse industry $1 billion annually, with an incidence of 8.5% to 13.7%.(1) Most often the source of lameness is the distal limb, as studies at worldwide racetracks have shown.(1) About 60% of lameness problems in horses are related to osteoarthritis (OA). For example: The U.S. horse population is currently estimated to be 7.3 million according to the American Veterinary Medical Association in 2010. This means that greater than 4 million horses are affected by OA. Considering direct and indirect medical expenses, the cost of one horse suffering from OA per year amounts to $15 000.(2) Thus articular disease constitutes the largest, single economic loss to the equine industry and arthritic pain represents a serious animal welfare concern.(3)

2.1.1 Pathogenesis of osteoarthritis

The definition of osteoarthritis is the degeneration of articular cartilage and typically features such as matrix fibrillation, fissures, ulceration and full-thickness loss of cartilage are present.(4) Specific mechanisms are responsible for the pathogenesis of OA. A defective cartilage with abnormal biomechanical properties may be one of the causes of OA. So the cartilage fails under normal loading conditions. Abnormal changes in the subchondral bone are the second mechanism for the pathogenesis of OA. Subchondral bone typically undergoes remodeling as a reaction to exercise or changes in load. It is also possible that the bone increases its density to a pathological level, which results in a stiffer bone. As a consequence the cartilage may break down. The third mechanism is a normal cartilage exposed to abnormal pressure. Abnormal forces overwhelm the normal metabolic repair mechanisms of the articular cartilage. Failure of the cartilage is then the ultimate consequence. Abnormal mechanical loads may result in micro damage of the cartilage or in a single traumatic event. Micro damage accumulates over a long time and then finally leads to the break down of the cartilage, if the normal repair process of the tissue is overwhelmed. A single traumatic event, such as an articular fracture immediately

leads to failure without a chance for repair. The correlation of the disease severity and the involvement of multiple joint tissues is often the case in OA. So the etiology is multifactorial. At some stage of OA, some degree of abnormal mechanical loads and metabolic tissue failure will be found in combination.(5) A decreased concentration of proteoglycans (PGs), potential changes in the size of collagen fibrils and aggregation of PGs, increased water content as well as increased synthesis and degradation of matrix macromolecules with disorganization of the collagen network are some of the earliest changes that occur in OA. They eventually cause the cartilage to be less resistant to stress, because they lead to breakdown and decreased content of the PG matrix. This results in ulceration with inflow of PGs into the synovial fluid with decreased water content of the cartilage. During the progression of the OA, collagen, PG and water content continue to be reduced, while the collagen network becomes heavily disrupted.(6)

2.1.2 The distal interphalangeal joint

Each joint can be affected by OA and there are often multiple joints affected in one horse at the same time. Depending on breed, age and use of the horse individual joints may be more often affected. Twenty-five percent of racing Thoroughbreds experience metacarpo/metatarsophalangeal joint pain.(7) In Thoroughbred racehorses the metacarpophalangeal joint is particularly susceptible to OA and injuries because it is a high-motion condylar joint that receives high loads during racing.(8) In Warmbloods for example a common site for OA is the distal interphalangeal joint (DIPJ).(9)

The DIPJ is a complex structure consistent not only of the articulation between the middle and distal phalanges with it`s collateral ligaments, but also the articulation with the navicular bone. The DIPJ also has a close association with the distal sesamoidean impar ligament (DSIL), the collateral sesamoidean ligaments (CSL), the navicular bursa and the deep digital flexor tendon (DDFT). The DIPJ is a classical hinge joint. There are three planes in which the DIP joint can move: flexion and extension in the sagittal plane, lateromedial movements in the frontal plane and rotating and sliding in the transverse plane. The collateral ligaments of the DIPJ, the DDFT, the distal digital annular ligament, the DSIL and the CSL all restrict the joint's

ability to move. The degree of sliding and axial rotation within the DIPJ are linked to a possible predisposition of the horse to DIPJ injury.(10)

DIPJ disease is often associated with other conditions of the foot and rarely occurs as an isolated condition.(11) The DIPJ load distribution and range of movements are influenced by two important factors related to the foot trimming in horses: 1) Medio-lateral foot imbalance results in changes in the weight distribution in the foot and also affects more proximally located structures especially the articulations.(11) 2) Dorso-palmar foot balance (the angle at which the hoof meets the ground) is often altered. A negative or positive palmar angle may influence the load on the structures located on the palmar aspect of the limb. These loads may then be altered for example as part of the management regime of conditions such as navicular disease and laminitis.(11)

The anatomical configuration and mechanical load distribution on the DIPJ may alter, if there is either a medio-lateral or a dorso-palmar imbalance. (11) This may also result in changes in the joint volume, i.e. the joint synovial space, which would be of little significance in the normal joint with negative intra-articular pressure. However, in cases with joint effusion and an increased joint fluid volume and therefore direct pressure on the cartilage, imbalance of the hoof could result in an increase in the intra-articular pressure, therefore contribute to damage to articular cartilage and ultimately result in lameness.(11)

2.1.3 Lameness associated with the DIPJ

Lameness associated with the DIPJ may be acute or chronic. Even though it can occur in both, it is more common in forelimbs than in hindlimbs. Horses with unilateral disease show a clear lameness, but those with bilateral lameness may be evaluated because of poor performance (e.g. shortened stride, reluctance to jump).

The DIPJ is often effused when there is disease, however also clinically sound horses can show a distention of this joint. So this finding is not pathognomonic for DIPJ pain. Chronic distention does reflect synovitis and it is possible that it can predispose to low-grade instability of the joint. The dorsal proximal out-pouching of the joint capsule can be palpated just proximal to the coronary band dorsally. When distention of the joint capsule is present, ballottement of fluid from medial to lateral of the dorsal midline should be possible. Flexion or rotation of the distal limb joints can

cause pain. To what degree lameness occurs depends on what pathological change is present and if it is unilateral or bilateral. Severe lameness may be the result of trauma to one of the supporting soft tissue structures of the joint. Distal limb flexion or rotation of the distal limb joints can emphasize lameness. Especially on a hard surface, lameness is often worse on a circle, with the lamest limb either on the inside or outside of the circle.

Pain associated with the DIPJ often improves after a palmar digital nerve block and sometimes is fully eliminated. Intraarticular analgesia of the DIPJ is not exclusive for pain that affects the joint itself. Also, pain originating from the navicular bone, the DSIL, the bursa, the CSL and the distal DDFT can result in a positive joint block. Lameness caused by primary joint pain usually improves very rapidly and substantially after intraarticular analgesia. If lameness is still apparent after 5-10 minutes, the joint is unlikely the primary source of pain. With time and diffusion of the local anesthethic agent lameness attributed to structures associated with the DIPJ may however improve. It is, for example, possible that intraarticular analgesia of the joint may not completely relieve pain associated with a primary injury of one of the collateral ligaments of the DIPJ. However, improvement may be seen if there is concurrent synovitis or osteoarthritis. (10)

2.1.4 Diagnostic imaging

Diagnostic imaging particularly radiography and ultrasonography are the next steps in confirming the cause of lameness. Degenerative joint disease of the DIPJ is frequently associated with little, if any, radiographic changes in the early stage. These changes include periarticular and periosteal osteophytes on the proximal articular margin of the distal phalanx, on the disto-dorsal and/or disto-palmar/plantar aspects of the middle phalanx and slight irregularities and incongruity of the joint surfaces, particularly the articular surface of the extensor process. The best way to spot radiographic abnormalities are on latero-medial and oblique views. (12) Whatever has caused the OA in the first place, it leads to thinning of the articular cartilage, especially in areas of high load. This cartilage thinning can be recognized radiographically as narrowing of the joint space. Unfortunately only the more advanced stages of the disease show the narrowing of the joint space and periarticular osteophytes and enthesiophytes radiographically. Another common

feature of OA is joint capsule thickening, be it with or without metaplasia. Radiographically, these changes are not observable. (13)

Ultrasound evaluation of articular cartilage is very angle dependent. Because it cannot assess the weight-bearing surfaces and because the ability to image structures situated in the hoof capsule is hard, the use of ultrasound in horses is mainly limited to evaluation of joint effusion, synovial proliferation, collateral ligament tears at their origin, DDFT lesions in the pastern and limited areas of joint surfaces.(14) By using the frog and bulbs of the heel as a window, ultrasonography can be used to image the soft tissue structures within the hoof capsule. This simple practical method allows measurements for the digital cushion, DDFT, distal recess of the podotrochlear bursa and the DSIL. The flexor surface of the distal phalanx and distal sesamoidean bone can also be imaged. Unfortunately the frog only allows visualization of the central structures of the ventral foot and not the structures medial, lateral and dorsal to the frog as the hoof capsule is impenetrable by ultrasound and this technique is not frequently done.(15)

Even though nuclear scintigraphy has been useful in the identification of horses with trauma of the DIPJ capsule insertion and subchondral bone, it appears to be rather insensitive to the identification of OA in a less advanced state.(10)

Magnetic resonance imaging (MRI) of the DIPJ permits excellent evaluation of the articular cartilage, the subchondral bone and the soft tissue structures associated with the DIPJ. Because OA leads to thinning of the articular cartilage and this thinning can visually be appreciated as narrowing of the joint space, different studies have measured the cartilage thickness or the joint space width by MRI in different joints. It is a fact that cartilage imaging in humans is more established than in horses and small animals.(16) In a study in 2010 the cartilage thickness of specific areas of 20 metacarpophalangeal joints of 10 mature racing Thoroughbreds was measured on MRI and compared with the histological measurements. This study illustrated that the MRI (SPGR – FS sequence) allows clinically applicable, satisfactory assessment of articular cartilage thickness, structure and to a lesser extent, early biochemical alterations in the osteoarthritic equine metacarpophalangeal joint.(16) Another study, performed in 2012, drawed the conclusion that the delayed gadolinium-enhanced magnetic resonance imaging of cartilage (dGEMRIC) and T2 mapping are accurate techniques for measuring metacarpus/metatarsus (Mc3/Mt3) cartilage thickness at locations where the cartilage is not in direct contact with the proximal phalanx

cartilage. In this study 24 metacarpus/metatarsus cadaver joints were acquired from six healthy thoroughbred racehorses.(1) In this study the low cartilage thickness in the distal metacarpus/metatarsus cartilage and the limit of detection of the measuring device were study limitations.

2.1.5 MRI as gold standard for early diagnosis of OA

Early lesions in the articular cartilage generally do not show signs of pain or lameness due to the lack of nociceptive receptors in this type of tissue. This implies that cartilage damage can and does progress while no clinical signs such as lameness are yet apparent. It is therefore imperative to use modalities that can detect cartilage injury early, enabling pathologic conditions to be addressed before they have progressed and allowing timeous therapy to be instigated.(14) Traditionally, OA has been diagnosed by the secondary indicators of cartilage loss (inflammation, pain, osteophyte development, joint space narrowing) via radiographic examination (17), in which a planar X-ray is applied to access the presence or absence of osteophytes and the width of the joint space. Hence the determination of pathology is based on indirect measures of surrounding anatomical structures (17). Even though this is usually an effective approach, radiographs tend to be limited. They detect OA only at later stages of disease progression, as they do not have the ability to directly image soft tissues (17). Also, radiographs are insensitive to all biochemical changes, which are absolutely needed for early diagnosis and treatment of joint pathologies.

The early stages of cartilage degeneration in OA are often characterized by the loss of the PG components of the cartilage matrix (17). Unlike the uncharged collagen, PGs present a net negative charge in solution. This fixed charge density attracts sodium and other small positive ions, which in turn pull additional water via osmosis into the cartilage matrix, where they create a positive pressure inside the tissue that helps articular cartilage to resist compressive loading forces encountered during normal activities as for example walking and running. In the beginning, disruption of PGs can lead to swelling via increased osmotic pressure and is eventually followed by the loss of cartilage volume. It has been assumed that PG depletion and the concomitant degradation of the cartilage matrix are one of the initiating events of the pathologic process leading to OA.(17) This awareness of biochemical correlates of pathology has encouraged a growing interest in using the capabilities of magnetic

resonance imaging (MRI) in the assessment of biochemical changes in the hopes of early diagnosis and corresponding treatment of diseases such as OA. Being a noninvasive technique, MRI has distinct advantages, is able to assess cartilage morphology directly and has shown promise for the detection of soft tissue changes.(17)

Traditional MR imaging methods have principally shown morphologic changes of cartilage, which probably represent progressed stages of OA. Before such morphologic changes, however, there are biochemical and structural changes in the extracellular matrix that change the biomechanical characteristics of the tissue.(6) Besides, these conventional methods have been based on water content and sometimes on collagen content and orientation. More modern techniques have been invented to map various MR imaging parameters, evaluating PG content, collagen content and orientation, water mobility and regional cartilage compressibility. Amongst these newer techniques are delayed gadolinium-enhanced magnetic resonance imaging of cartilage (dGEMRIC) and T2 cartilage mapping.(6) Parametric mapping of cartilage necessitates post-processing of images to produce relaxation time-associated color-maps which provide a visual interpretation basis of the specific areas` relaxation times. This has been described in T2 and dGEMRIC techniques.(1)

In delayed gadolinium-enhanced MRI of cartilage (dGEMRIC), the negatively charged contrast agent gadopentetate dimeglumine (GD-DPTA^{2-}) is injected either intraarticularly or intravenously. This contrast agent permeates hyaline cartilage and disperses in an inverse relationship to the PG content of the cartilage. When the PG concentration is diminished because of cartilage degradation, as seen in OA, the gadolinium uptake increases as a result of the relative decrease in negative charge of the PG-depleted cartilage. This dGEMRIC technique has been found to be an excellent indicator of degenerative cartilaginous changes and that it correlates with mechanical properties of cartilage such as cartilage stiffness.(4) By post-processing dGEMRIC images and producing relaxation time color maps, parametric mapping of cartilage can be achieved. These maps provide a detailed visual representation of relaxation times within specific locations.(4)

Collagen is the other important organic component of cartilage. Collagen fibers are organised in a fashion to maximise the efficiency in the transmission of joint forces

and joint lubrication. Loss of this orientation is a hallmark feature of OA. MRI using T2-relaxation time mapping is sensitive for determining the amount of collagen, its water content and its orientation within the cartilage.(19, 20) Early degenerative changes in the extracellular matrix affect tissue hydration by both increasing the overall water content via osmosis and increasing the mobility of water. Increased signal on T2-weighted images have been found in cartilage swelling due to cartilage edema and increased water content.(21) Also focal areas of increased signal on T2-weighted images have been found to correspond to cartilage lesions upon arthroscopic evaluation.(17) Additionally there is a link between early OA changes in T2-weighted images and the changes in collagen content.(17) The advantages and disadvantages of dGEMRIC and T2-mapping for evaluating cartilage morphology are the following (6): While the dGEMRIC sequence shows pictures with high resolution and sensivity, the T2-mapping is very sensitive to collagen, water content and motion. The disadvantages are the delay before imaging, the need for a contrast agent and the possibility of nephrogenic systemic fibrosis in patients with kidney problems when using contrast agents. The problem concerning the T2 maps is probably the lower sensivity in detection of early degeneration.

In humans quantitative MR techniques such as T2 cartilage mapping and to a lesser extent dGEMRIC have rapidly developed in recent years and have been used to identify OA early in the disease process.(22, 23) Only a handful of quantitive MRI techniques have been reported in horses.(1, 4, 24-26) Recently it was shown that dGEMRIC and T2 cartilage mapping were accurate techniques for measuring cartilage thickness at the distal metacarpus/metatarsus 3 (1) and established that dGEMRIC T1 and T2 relaxation times were similar in fresh, chilled and frozen cadaver limbs. (26)

The result of the study from 2013 was, that the histomorphometric cartilage thickness measurements did not differ from MRI measurements using a selected inversion recovery sequence for dGEMRIC mapping, and a selected time to echo image for T2 mapping in the palmaro/plantaro-distal aspect of the distal Mc3/Mt3. This finding validates the use of dGEMRIC and T2 mapping for measuring cartilage thickness in locations where cartilage is not in close approximation to opposing adjacent cartilage in the Mc3/Mt3 of Thoroughbred horses.(1)

To ensure that the bone-cartilage interface and the cartilage surface of the dGEMRIC and T2-mapping sites are consistent with true anatomical areas, validation studies comparing MRI measurements to histological measurements as the gold standard are needed before the cartilage boundaries can be accurately identified and the cartilage itself can be reliably evaluated. This is especially true for a complex joint like the DIPJ, where the navicular bone surface at the palmar/plantar aspect of the DIPJ complicates the caudal joint contour contacting the distal P2.

2.1.6 Aims of the current thesis

The aim of this thesis was to validate that dGEMRIC and T2-mapping of joint cartilage are accurate techniques for measuring joint cartilage thickness in the distal P2 and proximal P3 cartilage.

The aims are as stated below:

1) To determine histological measurements of cartilage thickness at 11 pre determined sites in normal and diseased Warmblood cadaver joints.
2) To determine measurements of cartilage thickness of the 11 pre determined sites on dGEMRIC and T2 maps in normal and diseased cadaver joints.
3) To correlate the histological measurements of cartilage thickness with the measurements of cartilage thickness of the MRI images for normal and diseased cadaver joints.
4) To test the effect of cartilage disease state and site within the joint on cartilage thickness (histological and MR measurements).
5) To determine the joint space width at 9 locations in the DIPJ and comparing the measurements from the MRI with the histological ones.

The following hypotheses were made:

1) Inter observer agreement of histological and MR measurements will be optimal to excellent.
2) There will be a significant correlation between histological and MR cartilage thickness measurements.

3) Cartilage thickness will not significantly differ when measured on dGEMRIC than when measured on T2-maps.
4) Joint disease state and site will have a significant effect on cartilage thickness measurements. Diseased joint cartilage will be thinner than normal joint cartilage. P3 cartilage will be thinner than P2 cartilage.
5) The joint space width will not significantly differ when measured on dGEMRIC or measured on T2 maps. There will be a significant correlation between MRI and histological measurements too.

2.2 Material and methods

2.2.1 Horses

This is a prospective cross – selectional study on 12 Warmblood cadaver fore limbs of horses with a mean age of 15.2 ± 9.2 (6 - 32 years). All horses were euthanised for reasons unrelated to the musculoskeletal tract according to Swiss ethical standards. Warmbloods of any gender, with no age restrictions, showing no signs of lameness at a walk or trot were included in the study. A right or a left forelimb was randomly dissected from the body in the intercarpal joint. The limbs were refrigerated (4°C) until scanning.

2.2.2 MRI

The limbs were scanned within 24 hours after death at room temperature on different days over a period of 4 months. A vitamin E oil capsule was taped to the lateral aspect of the hoof and each limb was positioned on the scanner table with the dorsal hoof wall facing downwards and the toe facing towards the gantry. A TR 16 - channel knee coil was used and the distal interphalangeal joint of each forelimb was scanned using a 3 Tesla MRI scanner (Phillips Health Care, Zofingen, Switzerland).
A frontal localizer was run to identify the condylar and intercondylar sagittal slices of each distal interphalangeal joint. The pre contrast T1 relaxation time was measured using single slice inversion recovery spin echo sequences (TR 12 ms, TE 5.6 ms, field of view 100 x 100 mm, matrix 252 x 244, slice thickness 3 mm, receiver band width 131.6 Hz/pixel) for each lateral and medial mid condylar sagittal slice and the central inter condylar sagittal slice (sagittal groove positioned in the middle of distal P2). The T2 - mapping images were acquired using multi – slice, multi – echo, spin – echo sequences (TR 2000 ms, TE 6 x 13 ms, field of view 160 x 160 mm, matrix 380 x 311, slice thickness 2.5 mm, receiver band width 291.1 Hz/pixel). By placing a 21 gauge needle into the dorsal recess of the DIPJ, as much synovial fluid as possible was aspirated to minimise dilution of the Gd (Gadolinium) – $DTPA^{2-}$ and to minimize fluid – related sources of variability. Gd – $DTPA^{2-}$ (Magnevist, gadopentetate dimeglumine, Bayer Health Care Pharmaceuticals, Basel, Switzerland) was injected into the DIPJ at 0.05 ml in 5 ml saline solution (0.025 mmol/joint). After the injection the joints were manually flexed for 5 minutes to distribute the contrast medium in all

parts of the joint. The limbs were scanned again using the same mid and central inter condylar slices 120 minutes after the injection of the contrast medium. The T1 relaxation time measurements were repeated.

2.2.3 MRI image analysis

Three regions of interest (ROIs) were analysed for each mid condylar and the inter condylar slice as shown in Fig 1.

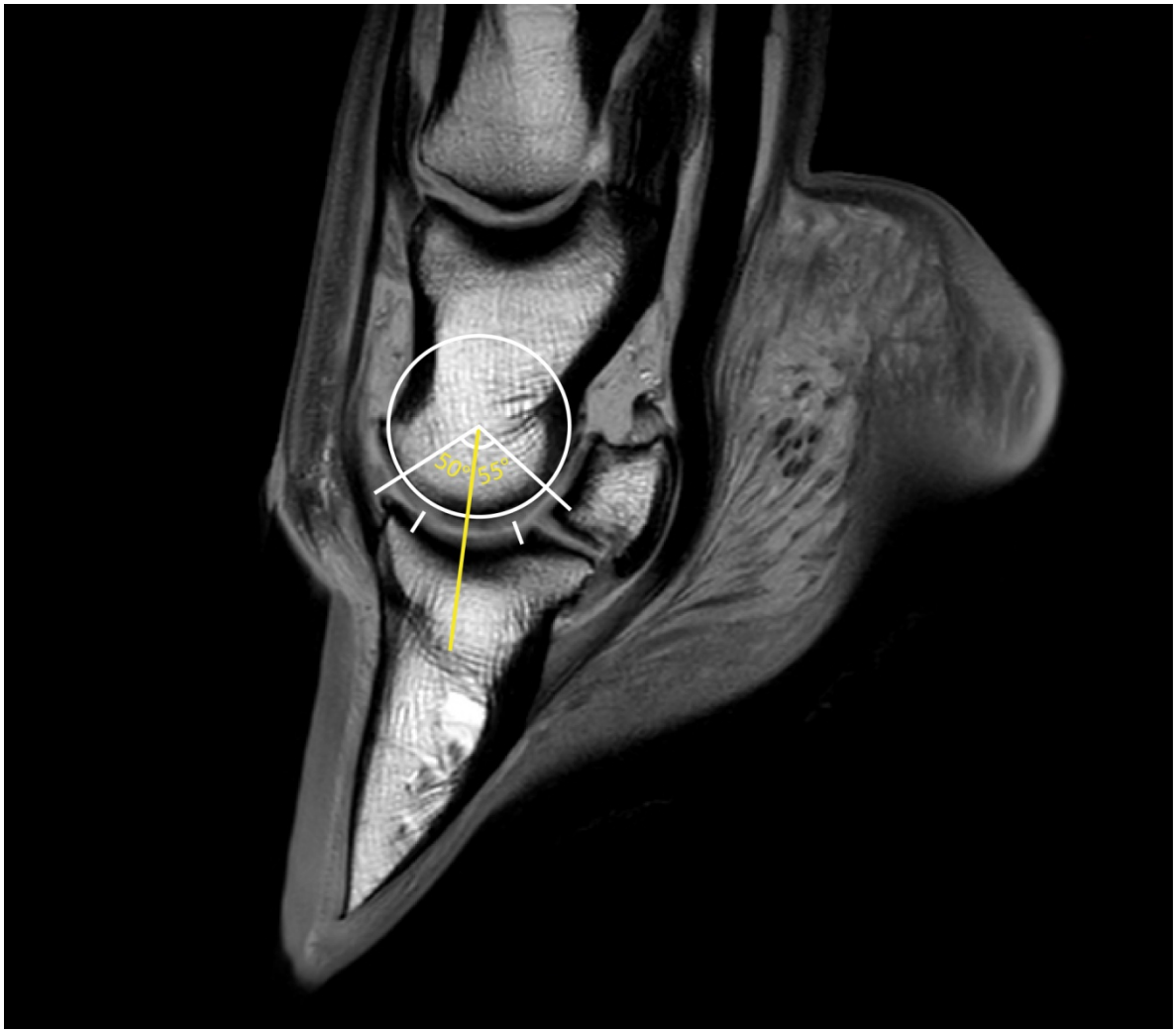

Fig.1: Site 2 was defined as the end of a vertical line through the rotation centre point of the DIPJ. Site 1 was defined at a 50° dorsal angle from the vertical line through the rotation centre point. Site 3 was defined at a 55° palmar angle from the vertical line through the rotation centre point.

Cartilage thickness was measured using an Osirix MD Version 7.5 workstation. Each image was zoomed into an optimal position where a translucent template (Fig 1) could determine the centrepoint in the middle of the condyles of the P2 and the midline that goes vertically through the DIPJ. The optimal window was found by using the windowing tool in the software and the sites were defined where the cartilage, the joint space, and the surface of the bone could best be identified. Two observers measured the thickness of the cartilage at each ROI three times and the mean ± standard deviation of each ROI of each observer was calculated. The second observer undertook the measurements one month later, but with the same settings.
For the joint space width (JSW) the cartilage thickness from the subchondral bone of proximal P3 and distal P2 was measured. The different sites of measurements in relation to the previous ROIs are shown below. (Table 1) A map of the different ROIs is provided in Fig 2.

Table 1: JSW and corresponding locations on P2/P3

JSW	Location	Correlated ROI position
A	lateral dorsal	1 and 10
B	lateral central	2 and 11
C	lateral palmar	3 and 12
D	middle dorsal	4 and 13
E	middle central	5 and 14
F	middle palmar	6 and 15
G	medial dorsal	7 and 16
H	medial central	8 and 17
I	medial palmar	9 and 18

2.2.4 Tissue harvesting

The DIPJs were disarticulated. Cartilage and subchondral bone cores (9 mm diameter) were cut from the distal aspect of P2 and from the proximal aspect of P3. A total of 11 cores were obtained per joint as shown in Fig 2a and 2b (yellow ROIs). A central 1000 µm thick osteochondral slice was cut from the core by using a saw and this slice was further processed for histological sections. Briefly the osteochondral samples were fixed in 4% paraformaldehyde for 48 hours, decalcified in 25% EDTA for 4 weeks, embedded in paraffin and sections were cut and stained with Haematoxylin and Eosin, Safranin O – Fast Green and Toluidine Blue.

In the MRI the cartilage thickness of the yellow and the blue ROIs (1 – 18) were measured:

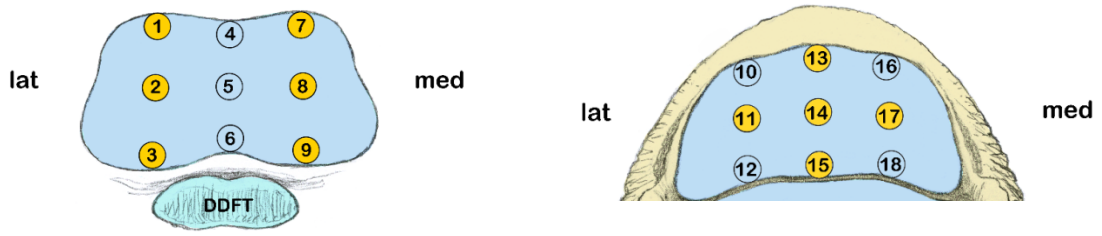

Fig.2a: P2 distal P3 proximal
DDFT = deep digital flexor tendon

In the histology only the 11 cores (yellow ROIs) were measured:

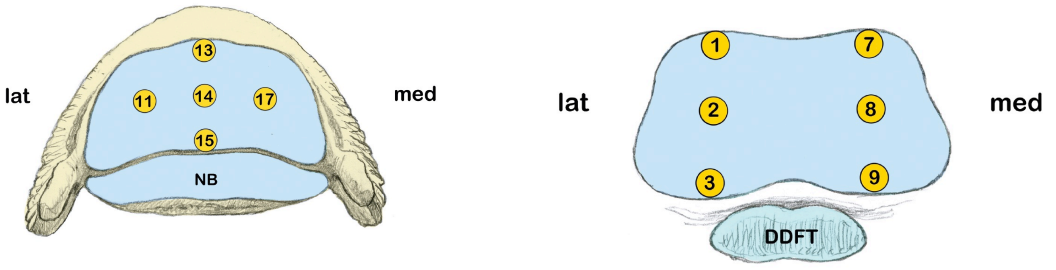

Fig.2b: P3 proximal P2 distal

2.2.5 Histological analysis

Three months after analysing the MRIs, the histological measurements of the cartilage thickness were obtained. Again two observers obtained the measurements with an interval of one month. A Leica DM LB2 light microscope equipped with a Leica DC 480 camera (Leica Microsystems Ltd, Heerbrugg, Switzerland) was used. The total thickness of the cartilage, the thickness of the calcified cartilage and the thickness of the hyaline cartilage were each measured three times (Fig 3). The mean ± standard deviation of the three measurements was calculated and used for the further analysis.

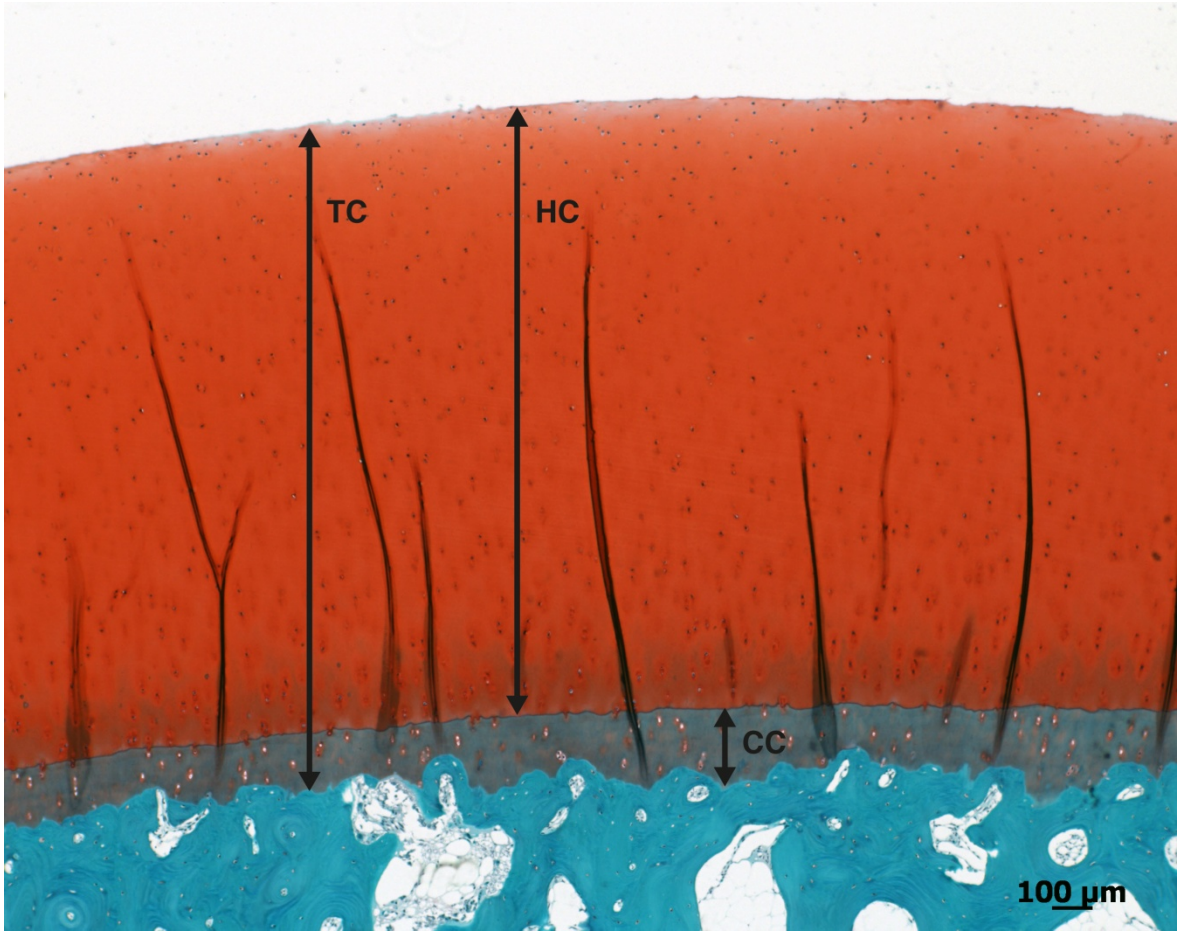

Fig.3: Safranin-O stain of normal cartilage. TC: total cartilage thickness, HC: hyaline cartilage thickness, CC: calcified cartilage thickness

Safranin-O stained sections were analysed and scored for degenerative changes by 3 blinded observers using a modified mankin scoring system. The histological sections of the different ROIs were scored on the basis of the following criteria shown in table 2. Briefly: Loss of staining (reflecting proteogylcan content) in the different cartilage zones, structure of the cartilage (presence of fibrillations, fissures, erosions), cell density of the cartilage and possible chondrocyte cluster formation. An overall cartilage score was given and the ROI was classified into 3 groups of differing degrees of cartilage change: Normal cartilage: 0 - 1.9 Mankin score; minimal to moderate cartilage change: 2.0 - 8.0 Mankin score; severe cartilage change: 8.1 - 16.0 Mankin score.

Table 2: Modified Mankin scoring system employed for articular cartilage assessment

Structure	
0	Normal
1	Fibrillation
2	Fissures
3	Erosion of 1/3 of depth of the hyaline cartilage
4	Erosion of 2/3 of depth of the hyaline cartilage
5	Full depth erosion of the hyaline cartilage
6	Full depth erosion of the hyaline and calcified cartilage
Chondrocyte density	
0	No decrease in cells
1	Focal decrease in cells
2	Multifocal decrease in cells
3	Multifocal confluent decrease in cells
4	Diffuse decrease in cells
Cluster formation	
0	Normal
1	< 4 clusters
2	≥ 4 but < 8 clusters
3	≥ 8 clusters
Safranin O - Fast Green staining	
0	Uniform staining throughout articular cartilage
1	Loss of staining in the superficial zone of hyaline cartilage
2	Loss of staining in the upper 2/3 of hyaline cartilage
3	Loss of staining in all of hyaline cartilage

2.2.6 Statistical analysis

A Kolmogorov – Smirnoff Test of normality was used to evaluate the distribution of the data. Results of parametric data were displayed as mean ± standard deviation (SD) and results of nonparametric data were displayed as median (range). For the statistical analysis the ROIs 1, 4, 7, 10, 13 and 16 were summarized into the horizontal dorsal cartilage zone, the ROIs 2, 5, 8, 11, 14, and 17 into the horizontal central cartilage zone and the ROIs 3, 6, 9, 12, 15 and 18 into the horizontal palmar cartilage zone. The ROIs 1, 2, 3, 7, 8, 9, 10, 11, 12, 16, 17, 18 were grouped into the sagittal condylar zone and the ROIs 4, 5, 6, 13, 14 and 15 were grouped in the sagittal intercondylar zone. The inter observer agreement of the cartilage thickness measurements (histological and MRI) and the mean overall cartilage Mankin scores were analysed using an intraclass correlation coefficients (ICC). Average measures were reported and ICCs > 0.7 were considered good, > 0.8 optimal and > 0.9 excellent. Associations between the mean histological cartilage thickness measurements (total cartilage, hyaline cartilage and calcified cartilage) and the MRI cartilage thickness measurements (dGEMRIC and T2) were investigated using Spearmans rho non-parametric correlations. Two generalized linear models with a gamma log link with cartilage thickness measured on dGEMRIC and T2 maps (mm) as dependent variables and bone (P2/P3), cartilage zones (sagittal condylar/intercondylar zones) and (dorsal/central/palmar) and cartilage disease (none/minimal-moderate/severe) as independent variables were performed. Data analysis was performed using the SPSS 21.0 software (SPSS INC, Chicago, USA). The level of significance was set at $P < 0.05$.

2.3 Results

Nine scores were lost during the histopathological processing resulting in data of 123 ROIs being included in the study.

Figure 4 shows histological sections of specimens with different lesions. The samples are stained with Safranin O – Fast Green to illustrate the pathological findings. The inter observer agreement was excellent (ICC = 0.973) for the overall mean Mankin scores.

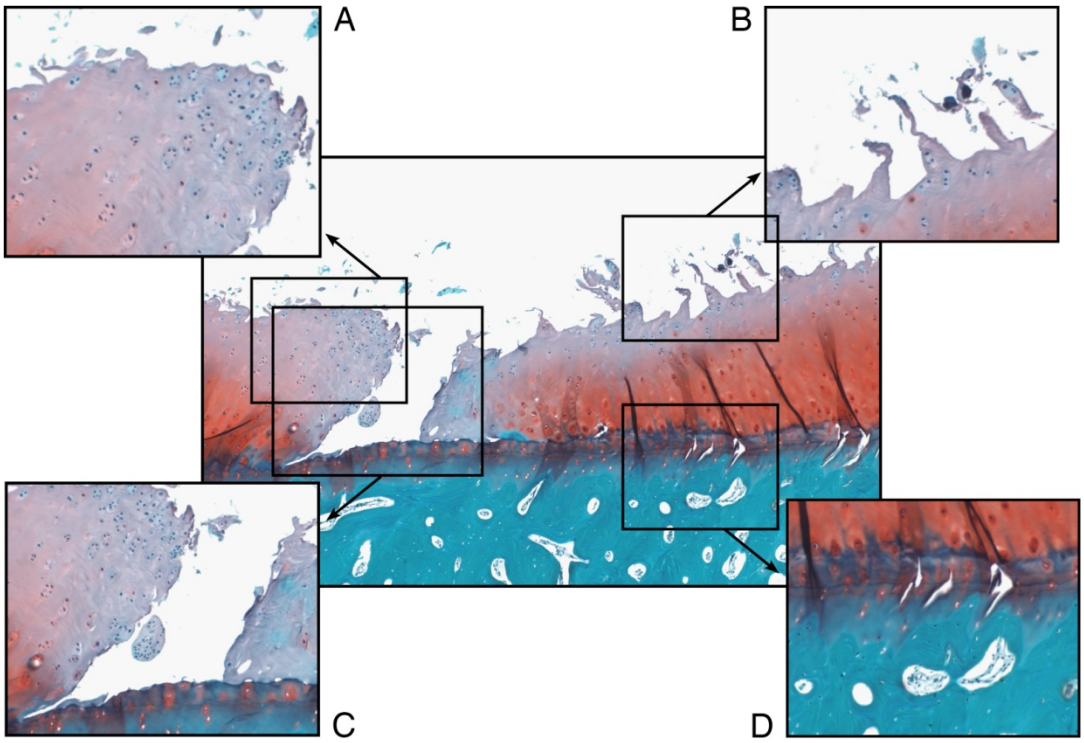

Figure 4: A: cluster formation of chondrocytes
B: multiple fibrillations and fissures in the superficial cartilage zone
C: full depth erosion of the hyaline cartilage
D: cracks in the calcified cartilage zone

MRI thickness measurements:

The inter observer agreement of the MRI cartilage thickness measurements was excellent (ICC = 0.953) for dGEMRIC and optimal (ICC = 0.835) for T2 maps. For the

JSW measurements the inter observer agreement was also excellent (ICC = 0.943) for dGEMRIC and optimal (ICC = 0.893) for T2 maps.

As shown in table 3 cartilage health had a significant effect on T1 cartilage thickness. Normal cartilage was significantly thicker than severely diseased cartilage and mildly to moderately diseased cartilage was also significantly thicker than severely diseased cartilage. Cartilage in the dorsal zone was significantly thinner than cartilage in the palmar zone. Cartilage thickness in the central zone was not significantly different from the cartilage in the palmar zone. In terms of significant difference in cartilage thickness it did not matter if the ROI was in the condylar groove or on the condyle or whether the ROI was on P2 or on P3.

Table 3: Median and range of T1 relaxation times of the independent parameters in the generalized linear models. 95% CI and p – values of the generalized linear models. Significant values are marked in bold.
Abbreviations: mod. = moderate, CI = confidence interval

Independent parameters	**Thickness in T1 (µm)**	**95% CI**	**P-value**
Intercept		6.828-7.048	**<0.001**
Normal cartilage	1253 (517-1791)	0.050-0.260	**0.004**
Mild – mod. cartilage disease	1179 (516-1974)	0.014-0.212	**0.023**
Severe cartilage disease	986 (519-2030)	-	-
P2	1121 (521-1791)	0.161-0.040	0.237
P3	1244 (346-2030)	-	-
Horizontal dorsal	950 (516-1791)	0.199-0.031	**0.007**
Horizontal central	1283 (346-2030)	0.008-0.160	0.075
Horizontal palmar	1102 (532-1974)	-	-
Sagittal condylar	1161 (346-2030)	0.067-0.154	0.438
Sagittal intercondylar	1164 (516-1974)	-	-

On T2 maps normal cartilage and mildly to moderately diseased cartilage was thicker than severely diseased cartilage (shown in table 4). On T2 maps, cartilage located on the condyle was thinner than cartilage located in the condylar groove. Whether the cartilage was located on P2 or P3 did not significantly affect the cartilage and neither did the location (dorsal/central/palmar).

Table 4: Median and range of T2 relaxation times of the independent parameters in the generalized linear models. 95% CI and p – values of the generalized linear models. Significant values are marked in bold.
Abbreviations: mod. = moderate, CI = confidence interval

Independent parameters	Thickness in T2 (µm)	95% CI	P-value
Intercept		6.838-7.056	**<0.001**
Normal cartilage	1095 (569-1944)	0.050-0.256	**0.003**
Mild – mod. cartilage disease	1113 (421-2177)	0.044-0.238	**0.004**
Severe cartilage disease	844 (311-1658)	-	-
P2	1032 (311-2177)	0.131-0.066	0.527
P3	1156 (421-1965)	-	-
Horizontal dorsal	1078 (468-1670)	0.091-0.074	0.842
Horizontal central	1112 (311-2177)	0.014-0.151	0.103
Horizontal palmar	1088 (590-1796)	-	-
Sagittal condylar	1037 (311-2177)	0.228-0.011	**0.030**
Sagittal intercondylar	1162 (468-1944)	-	-

Tables 5, 6 and 7 showing descriptive T1 and T2 data of the independent variables included in the generalized linear model are shown in the appendix.

MRI joint space width measurements:

The median (range) of the normal joint space width of the distal interphalangeal joint is shown in table 8 for T1 and T2 images. Generally the JSW is smaller measured on T2 maps than on T1 maps.

Table 8: Median and range of T1 and T2 of the independent parameters in the generalized linear models divided by cartilage health.
Abbreviations: mod. = moderate, n = number of samples

Independent parameters	T1 (µm)	n	T2 (µm)	n
Normal cartilage	3585 (2030-4545)	29	3121 (1785-4389)	29
Mild – mod. cartilage disease	3723 (1851-5374)	53	3210 (1428-4471)	53
Severe cartilage disease	3472 (2064-4666)	12	3338 (1882-4739)	12

Histological cartilage thickness measurements:

The inter observer agreement of the cartilage thickness measurements in histology was excellent (ICC = 0.922) for the total cartilage, excellent (ICC = 0.939) for the hyaline cartilage and good (ICC = 0.712) for the calcified cartilage.

Cartilage health status significantly affected the TC cartilage thickness, where normal and mildly to moderately diseased cartilage was significantly thicker than severely diseased cartilage (Table 9). The same was true for hyaline cartilage (Table 10). However, cartilage health did not affect the calcified cartilage thickness (Table 11).

The cartilage of P2 was significantly thinner than the cartilage of P3 for TC as well as for HC. The central areas were significantly larger than the palmar ones in TC and HC, but there is no significant difference between the dorsal and palmar zone.

Table 9: Median and range of TC of the independent parameters in the generalized linear models. 95% CI and p – values of the generalized linear models.

Abbreviations: mod. = moderate, CI = confidence interval, TC = total cartilage

Independent parameters	**Thickness in TC (µm)**	**95% CI**	**P-value**
Intercept		7.263-7.440	**<0.001**
Normal cartilage	1895 (1068-3263)	0.223-0.389	**<0.001**
Mild – mod. cartilage disease	1950 (999-3121)	0.190-0.346	**<0.001**
Severe cartilage disease	1429 (885-2499)	-	-
P2	1662 (969-3263)	0.240-0.081	**<0.001**
P3	2127 (885-3165)	-	-
Horizontal dorsal	1806 (10192590)	0.104-0.027	0.251
Horizontal central	2089 (885-3165)	0.068-0.201	**<0.001**
Horizontal palmar	1558 (969-3263)	-	-
Sagittal condylar	1776 (885-3263)	0.112-0.063	0.581
Sagittal intercondylar	2083 (999-3121)	-	-

Table 10: Median and range of HC of the independent parameters in the generalized linear models. 95% CI and p – values of the generalized linear models.
Abbreviations: mod. = moderate, CI = confidence interval, HC = hyaline cartilage

Independent parameters	Thickness in HC (µm)	95% CI	P-value
Intercept		7.130-7.316	**<0.001**
Normal cartilage	1714 (1019-2961)	0.263-0.438	**<0.001**
Mild – mod. cartilage disease	1731 (767-3035)	0.213-0.378	**<0.001**
Severe cartilage disease	1270 (695-2237)	-	-
P2	1477 (695-2961)	0.264-0.097	**<0.001**
P3	1992 (767-3035)	-	-
Horizontal dorsal	1571 (876-2307)	0.106-0.033	0.300
Horizontal central	1952 (787-2807)	0.087-0.226	**<0.001**
Horizontal palmar	1391 (695-3035)	-	-
Sagittal condylar	1590 (695-2961)	0.125-0.059	0.483
Sagittal intercondylar	1954 (767-3035)	-	-

Table 11: Median and range of CC of the independent parameters in the generalized linear models. 95% CI and p – values of the generalized linear models.
Abbreviations: mod. = moderate, CI = confidence interval, CC = calzified cartilage

Independent parameters	Thickness in CC (µm)	95% CI	P-value
Intercept		5.173-5.389	**<0.001**
Normal cartilage	202 (84-384)	0.027-0.176	0.147
Mild – mod. cartilage disease	192 (69-406)	0.095-0.096	0.978
Severe cartilage disease	202 (108-288)	-	-
P2	196 (84-514)	0.027-0.167	0.153
P3	199 (69-384)	-	-
Horizontal dorsal	174 (69-406)	0.140-0.022	0.149
Horizontal central	208 (77-514)	0.012-0.149	0.096
Horizontal palmar	199 (84-352)	-	-
Sagittal condylar	196 (77-514)	0.183-0.030	0.157
Sagittal intercondylar	201 (69-384)	-	-

Table 12, 13 and 14 shows descriptive data of the thickness of the total cartilage, hyaline cartilage and calcified cartilage and can be found in the appendix.

Histologic joint space width measurements:

The histological JSW measuring of the opposing TC, CC, and HC are shown in table 15.

Table 15: Median and range of the JSW measurements of TC, CC and HC of the independent parameters in the generalized linear models. JSW measurements in the different health zones.
Abbreviations: mod. = moderate, n = number of samples, TC = total cartilage, HC = hyaline cartilage, CC = calcified cartilage

Independent parameters	**TC (µm)**	**n**	**HC (µm)**	**n**	**CC (µm)**	**n**
Normal cartilage	4464 (3784-4631)	2	4080 (3581-4174)	2	379 (251-460)	2
Mild – mod. cartilage disease	4473 (1951-5649)	11	4046 (1778-5061)	11	434 (271-745)	11
Severe cartilage disease	4114 (2890-4677)	4	3704 (2633-4386)	4	388 (237-500)	4

Correlations between histological and MRI data:

There was a significant correlation between the T1 cartilage thickness measurements and the histological cartilage thickness measurements. The same was true for the T2 cartilage thickness measurements and the histological cartilage thickness measurements.

T1 cartilage thickness measurements correlated better with histological measurements (TC and HC) than T2 cartilage thickness measurements (TC and HC). For both T1 and T2 images the correlation coefficients were slightly higher for TC measurements than HC measurements on histological slides.

Table 16: Correlations between mean T1, mean T2 and mean TC, HC, CC
Abbreviations: r = Spearman` s rho correlation coefficient value; p = p – value

	Mean T1	Mean T2
Mean TC	r = 0.432; p <0.001	r = 0.350; p <0.001
Mean HC	r = 0.420; p <0.001	r = 0.339; p <0.001
Mean CC	r = 0.296; p <0.001	r = 0.207; p <0.001

Because of the low number of samples in the JSW measurements (2 healthy JSW samples, 4 severely diseased JSW samples), only the correlations of the mild – moderate diseased cartilage JSWs (totally 11) were calculated.

The significant Spearman`s correlation coefficient value of 0.491 confirms that there was a good correlation between the mean T1 and the mean TC thickness (p = 0.004) and between the mean T1 and the mean HC thickness (r = 0.427; p = 0.013).

The mean T2 cartilage thickness measurement also correlated with the mean TC (r = 0.366; p = 0.036), however there was no correlation between T2 and mean HC (r = 0.332; p = 0.059). Again the correlations of the mean T1 JSW measurements with the TC and HC were stronger than the correlations of the T2 JSW measurements and the TC and HC.

2.4 Discussion

The significance of this study is linked to the questions 1) if there was a significant correlation between histological and MR cartilage thickness measurements and 2) if cartilage thickness was better correlated to dGEMRIC (T1) or T2 measurements? Another important hypothesis was, that the joint disease state and site may have a significant effect on cartilage thickness measurements. This study found that the histological cartilage thickness measurements significantly correlated with the dGEMRIC (T1) and the T2 cartilage thickness measurements. The correlations between the T1 measurements and the histological measurements were always better than the T2 measurements compared to the histological measurements.

Because the contrast between the bright articular cartilage and the dark synovial fluid and the subchondral bone is high, cartilage could better be identified in T1 than in the T2 sequence, where the grey cartilage often only had low contrast to the dark subchondral bone. On the T2 sequences the low signal cartilage has been seen as a progressive continuum of the low signal subchondral bone. An equine study by Olive et al. using T1- and T2 weighted sequences for cartilage assessment in the DIPJ also considered the T1 sequence as the best for the contrast between both, the synovial fluid (replaced by saline in this study) and the subchondral bone plate compared to the cartilage.(27) In that study, however, the cartilage plates of P2 and P3 could not be clearly separated on T1 and T2 sequences when there was a very narrow joint space. This may also be attributed to the use of a low-field magnet for aquisition of the images, which resulted in less image resolution. To separate the two cartilage surfaces, the use of traction has been described in a human study. With traction the opposite cartilages could be better evaluated in the human knee.(1, 28) This technique could also be considered in future when evaluating the cartilages in the equine DIPJ using T1 or T2 mapping.

Because the thickness of normal equine metacarpophalangeal joint cartilage is minimal compared to humans, it is not possible to see surface lesions unless a large amount of synovia is present to provide an interface between the two opposite joint surfaces.(14) Irregularities in the cartilage surfaces appeared quite often and could not always been classified into erosions or image artefacts. However, these cartilage

cavities were identified as areas that were isotense to synovial fluid and had low intensity on T1 weighted images and high signal in T2 weighted images.

In humans, quantitative MR techniques such as dGEMRIC and T2 cartilage mapping have rapidly developed in recent years and can identify OA in early disease stages.(22, 23) The dGEMRIC technique has also been described as successful in the evaluation of cartilage regeneration after cartilage grafting techniques in human reports.(29-31) It was shown that dGEMRIC and T2 cartilage mapping were accurate techniques for measuring equine cartilage thickness at the distal (Mc3/Mt3). (1) The normal cartilage of the distal Mc3/Mt3 is approximately 1 mm thick (1) vs. the average thickness of the DIPJ cartilage of 2.1 – 3.1 mm (27). The metacarpophalangeal joint has also more complex anatomic constraints and a more rounded articular surface compared to the DIPJ, so similar comparisons cannot be made.(27) However, our T1, T2 as well as the histological measurements showed that the joint disease state has a significant effect on cartilage thickness measurements. The severely diseased cartilage was always the thinnest. This was expected because one of the consequences of OA is a thickness loss of the cartilage.(1). Irrespective of the aetiological factor of OA, it finally leads to thinning of the articular cartilage, especially in areas of high load. This cartilage thinning can be recognized radiographically as narrowing of the joint space. (13) On T1 the severely diseased condylar cartilage was thinner than the intercondylar one, in normal cartilage this was not the case. It can be assumed that the weight – bearing locations as the condyles are more affected by the cartilage loss, occurring in OA, than the other areas within the joint.

Whether a ROI was located on the condyle or in the condylar groove had a significant effect on the T2 thickness measurements. Our results on T2 showed a significantly thinner cartilage in the condylar than in the intercondylar area. The difference was most pronounced when the cartilage was severely diseased. The T2 map is sensitive for determining the amount of collagen, its water content and its orientation within the cartilage.(19, 20) The above mentioned study detected that the collagen content was higher in areas with intermittent peak loading.(32) So it can be assumed that the constant weight - bearing condyles had less collagen than the intercondylar zones and the joint margins. A loss of collagen can be seen as a focal signal loss on T2

sequences. A study measuring the cartilage thicknesses at different ROIs in the DIPJ, too, showed that there is an abrupt thinning of cartilage at the most abaxial palmar aspects of the distal phalanx, which should not be confused with an erosion.(27)

In the T1 and T2 images the normal cartilage is thinnest in the dorsal and thickest in the central zone. Compared to the histology there is a good agreement. The thickest cartilage is also centrally located in histology, the thinnest cartilage is always palmar, independent of the health status. These results correspond very well to the results of an equine study, assessing the DIPJ cartilage using low-field magnetic resonance imaging.(27) This study describes in detail that the cartilage is centrally on the distal phalanx significantly thicker palmary and get progressively thinner dorsally towards the extensor process. On the middle phalanx the cartilage was mildly thicker palmarocentrally in the sagittal groove and then thickness reduced progressively abaxially and dorsally.(27) The above mentioned study supports also our hypothesis that P2 had a thinner cartilage than P3. It can be hypothesized that during the different phases of walk or trott the P3 has more pressure to bear than the P2. In consequence the cartilage of the P3 has become thicker as an adaptation to these circumstances.

MRI measurement of cartilage is important in experimental and clinical OA.(16) Our results demonstrate that cartilage thickness of the DIPJ can be measured with reasonable accuracy, although cartilage thickness was constantly underestimated on MR images (T1 and T2 images). The same facts apply also for the JSW measurements. We can only speculate why our MRI thickness measurements were smaller than the histological measurements. A reason could be the oblique orientation of the articular surfaces of P3/P2, causing volume averaging. Cartilage thickness measurement differences could also be caused by slice thickness.(16) For the human knee a slice thickness of 1.5 mm with isotropic 0.3 mm in-plane resolution is recommended (34), but this is not realistic in live equine patients that often require multiple imaging sequences of the affected joint and additional sequences of other regions, like the opposite limb for comparison (16). In our study a 2.5 mm slice thickness was used in the T2 and a 3 mm slice thickness in T1. These thicknesses were the same as in previous equine studies.(35)

The results are in contrast to previous studies examining the equine carpus.(16) Previous studies reported an overestimation of cartilage thickness when the cartilage thickness is < 1mm. Limitations such as voxel size and in-plane resolution combined with the convex shape of the condyles causing volume averaging are possible explanations for that.(16) In addition the histological processing could also have an effect on the cartilage dimensions. Because the range of our healthy cartilage thicknesses (1068 – 3263 um) is quite higher than 1 mm, an overestimation due to the small thickness was not expected.

It was encouraging that in our study the inter observer agreement of MRI measurements was excellent in T1 (ICC = 0.953) and optimal in T2 (ICC = 0.835). In the histology the agreement was good (calcified cartilage ICC = 0.712) to excellent (total cartilage ICC = 0.922; hyaline cartilage ICC = 0.939). Because the width of the calcified cartilage is very thin compared to the hyaline and total cartilage and the tideline between the calcified and the hyaline cartilage is mostly wavy, the discrepancy of the measurements among the observers could be expected.

We chose twelve 6-32 year old Warmblood horses for our study, because horses in this age range were likely to have a range of normal cartilage, mild OA and severe OA in the DIPJ. One limitation of our study was the relatively low number of horses and the examination of only one foreleg of a horse. The comparison of the contralateral limb could have given interesting information about the health status and the thicknesses of the cartilage. Because of different factors such as time, expenses and complexity of the study we decided to collect and process our samples within one year and therefore we had to restrict the dimension of the study. However in a clinical setting the examination of the contralateral limb in MRI is absolutely essential. For the same reasons only 11 cores were obtained from the distal P2 and the proximal P3 for the histological processing compared to the 18 ROIs in the MRI. So a comparison of the cartilage thicknesses in MRT versus histology was only made in 11 ROIs per leg. Besides that with the histology 9 scores were lost during the processing procedure of the specimens.
The small number of samples in the JSW measurements only allowed descriptive statistics to be performed in the healthy and severely diseased cartilage zones. However, the mild-moderate diseased JSW locations allowed a statistical analysis

and showed good correlations between MRI and histology data (s. above). A further limitation in the JSW measurements is the fact, that the two opposite cartilages were added together from the appropriate histological samples, thus the space between the two opposing cartilage surfaces measured on MRI was missing on histology. So a little discrepancy between MRI and histology was expected.

In our study, breathing – related movements of the limb were absent. This could be a disturbing factor and reduce the quality of the images in live horses.(16) However it should be possible to fix the limb as to limit most motion artefacts.(16) In the clinical situation, a horse would be anesthetized for the MRI examination. Absence of weight bearing allows assessment of the articular cartilage surface due to interspacing synovial fluid. So the contrast is improved.(27) In contrast to that, in a standing horse the joint space is reduced and the opposing cartilage surfaces are in contact. Moreover the fact, that the resolution of MR images obtained in standing magnets are generally of lower strength (< 0.3 tesla), result in poorer image quality. Mapping sequences cannot be used due to the small slice thickness needed which would result in long scanning times and potential motion artifacts associated with this. In our study a 3 tesla MRI scanner was used. A high – field MRI (≥ 1 tesla) is still regarded as the modality of choice to evaluate the articular cartilage of horses, because a more appropriate method does not exist yet.(14) A human study comparing 3 tesla with 1.5 tesla images, reported superior cartilage thickness measurements when using the higher field strength magnet.(38) The use of thinner slices for MRI scans in our study would have resulted in a lower signal – to – noise ratio however would have required more time. Findings in a study evaluating the human knee cartilage volume showed that there was only little difference in the human tibial cartilage volume when slice thicknesses were increased from 1.5 to 7.5 mm.(39) Because of the different curvature and thicknesses of the cartilage, the DIPJ cannot directly be compared with the human knee, but it can be assumed that our slice thicknesses (2.5 – 3 mm) will give reliable results.

In conclusion, findings in this study indicated that the histological cartilage thickness measurements correlated well with the dGEMRIC (T1) and T2 cartilage thickness measurements.

The correlation was stronger between the T1 measurements and the histological cartilage thickness than between the T2 measurements and the histological cartilage thickness.

As expected increasing degree of OA lead to a decreasing cartilage thickness. Normal cartilage was significantly thicker than severely diseased cartilage, and mildly diseased cartilage was also significantly thicker than severely diseased one.

There were regional differences in cartilage thickness depending on the cartilage site within the joint. So, the cartilage of P2 is thinner than the P3 one and the central areas are larger than the palmar zones. Finally is the condylar cartilage thinner than the intercondylar one.

The JSW correlations of the mean T1 measurements with the TC and HC were stronger than the correlations of the T2 measurements and the TC and HC. Generally the JSW is smaller measured on T2 maps than on T1 maps.

Our findings finally show that both, dGEMRIC and T2-maps, are reliable to measure cartilage thickness in normal and degenerated cartilage in areas of opposing or non-opposing cartilage surfaces.

2.5 References

1. Carstens A, Kirberger RM, Dahlberg LE, Prozesky L, Fletcher L, Lammentausta E. Validation of delayed gadolinium-enhanced magnetic resonance imaging of cartilage and T2 mapping for quantifying distal metacarpus/metatarsus cartilage thickness in Thoroughbred racehorses. Vet Radiol Ultrasound. 2013;54(2):139-48.

2. Oke S, McIlwraith CW, Moyer W. Review of the economic impact of osteoarthritis and oral joint-health supplements in horses. Joints AAEP. 2010.

3. de Grauw JC. Molecular monitoring of equine joint homeostasis. Veterinary Quarterly. 2011;31(2):77-86.

4. Carstens A, Kirberger RM, Velleman M, Dahlberg LE, Fletcher L, Lammentausta E. Feasibility for mapping cartilage T1 relaxation times in the distal metacarpus3/metatarsus3 of thoroughbred racehorses using delayed gadolinium-enhanced magnetic resonance imaging of cartilage (dGEMRIC): normal cadaver study. Veterinary Radiology & Ultrasound. 2013;54(4):365-72.

5. Auer J, Stick J. Equine Surgery, Third Edition (2012); chapter 83: Synovial Joint Biology and Pathobiology, 1036-1055, David D. Frisbie, W.B. Saunders Company, Philadelphia

6. Choi J-A, Gold GE. MR imaging of articular cartilage physiology. Magnetic resonance imaging clinics of North America. 2011;19(2):249-82.

7. Bailey C, Reid S, Hodgson D, Bourke J, Rose R. Flat, hurdle and steeple racing: risk factors for musculoskeletal injury. Equine Veterinary Journal. 1998;30(6):498-503.

8. Neundorf RH, Lowerison MB, Cruz AM, Thomason JJ, McEwen BJ, Hurtig MB. Determination of the prevalence and severity of metacarpophalangeal joint

osteoarthritis in Thoroughbred racehorses via quantitative macroscopic evaluation. American journal of veterinary research. 2010;71(11):1284-93.

9. Wilke MM, Nydam DV, Nixon AJ. Enhanced early chondrogenesis in articular defects following arthroscopic mesenchymal stem cell implantation in an equine model. Journal of Orthopaedic Research. 2007;25(7):913-25.

10. Ross MW, Dyson SJ. Diagnosis and Management of Lameness in the Horse, Second Edition (2010); chapter 33: The Distal Phalanx and Distal Interphalangeal Joint, 349-355, Sue J. Dyson, Elsevier Health Sciences, Pennsylvania

11. Viitanen M, Wilson A, McGuigan H, Rogers K, May S. Effect of foot balance on the intra-articular pressure in the distal interphalangeal joint in vitro. Equine Veterinary Journal. 2003;35(2):184-9.

12. Butler J, Colles C, Dyson S, Kold S, Poulos P. Clinical radiology of the horse, Third Edition (2012); chapter 3: Foot, Pastern and Fetlock, 53-187, John Wiley & Sons, Oxford

13. Floyd A, Mansmann R. Equine podiatry, First Edition (2007); chapter 13: Pathologic Conditions Involving the Internal Structures of the Foot, 253-293, W. Rich, Elsevier Health Sciences, St Louis, Missouri

14. Pease A. Biochemical evaluation of equine articular cartilage through imaging. Veterinary Clinics of North America: Equine Practice. 2012;28(3):637-46.

15. Sage A, Turner T. Ultrasonography of the soft tissue structures of the equine foot. Equine Veterinary Education. 2002;14(4):221-4.

16. Olive J, D'ANJOU MA, Girard C, Laverty S, Theoret C. Fat-suppressed spoiled gradient-recalled imaging of equine metacarpophalangeal articular cartilage. Veterinary Radiology & Ultrasound. 2010;51(2):107-15.

17. Taylor C, Carballido-Gamio J, Majumdar S, Li X. Comparison of quantitative imaging of cartilage for osteoarthritis: T2, T1ρ, dGEMRIC and contrast-enhanced computed tomography. Magnetic resonance imaging. 2009;27(6):779-84.

18. Murray RC. Equine MRI, First Edition (2010); chapter 20: The foot and pastern, 491-512, Andrew Bathe, John Wiley & Sons, Chichester, West Sussex

19. Goodwin DW, editor Visualization of the macroscopic structure of hyaline cartilage with MR imaging. Seminars in musculoskeletal radiology; 2001.

20. Xia Y, Moody JB, Alhadlaq H. Orientational dependence of T2 relaxation in articular cartilage: A microscopic MRI (μMRI) study. Magnetic resonance in medicine. 2002;48(3):460-9.

21. Murray RC, Dyson S. Image interpretation and artifacts. Clinical Techniques in Equine Practice. 2007;6(1):16-25.

22. Gold GE, Burstein D, Dardzinski B, Lang P, Boada F, Mosher T. MRI of articular cartilage in OA: novel pulse sequences and compositional/functional markers. Osteoarthritis and Cartilage. 2006;14:76-86.

23. Potter HG, Black BR. New techniques in articular cartilage imaging. Clinics in sports medicine. 2009;28(1):77-94.

24. Domayer S, Welsch G, Nehrer S, Chiari C, Dorotka R, Szomolanyi P, et al. T2 mapping and dGEMRIC after autologous chondrocyte implantation with a fibrin-based scaffold in the knee: preliminary results. European Journal of Radiology. 2010;73(3):636-42.

25. Menendez M, Clark D, Carlton M, Flanigan D, Jia G, Sammet S, et al. Direct delayed human adenoviral BMP-2 or BMP-6 gene therapy for bone and cartilage regeneration in a pony osteochondral model. Osteoarthritis and Cartilage. 2011;19(8):1066-75.

26. Carstens A. Delayed gadolinium-enhanced magnetic resonance imaging and T2 mapping of cartilage of the distal metacarpus3/metatarsus3 of the normal Thoroughbred horse 2013. (Doctoral Dissertation)

27. Olive J. Distal interphalangeal articular cartilage assessment using low-field magnetic resonance imaging. Veterinary Radiology & Ultrasound. 2010;51(3):259-66.

28. Naish J, Xanthopoulos E, Hutchinson C, Waterton J, Taylor C. MR measurement of articular cartilage thickness distribution in the hip. Osteoarthritis and Cartilage. 2006;14(10):967-73.

29. Trattnig S, Mamisch TC, Pinker K, Domayer S, Szomolanyi P, Marlovits S, et al. Differentiating normal hyaline cartilage from post-surgical repair tissue using fast gradient echo imaging in delayed gadolinium-enhanced MRI (dGEMRIC) at 3 Tesla. European Radiology. 2008;18(6):1251-9.

30. Trattnig S, Marlovits S, Gebetsroither S, Szomolanyi P, Welsch GH, Salomonowitz E, et al. Three-dimensional delayed gadolinium-enhanced MRI of cartilage (dGEMRIC) for in vivo evaluation of reparative cartilage after matrix-associated autologous chondrocyte transplantation at 3.0 T: Preliminary results. Journal of Magnetic Resonance Imaging. 2007;26(4):974-82.

31. Bekkers J, Bartels L, Benink R, Tsuchida A, Vincken K, Dhert W, et al. Delayed gadolinium enhanced MRI of cartilage (dGEMRIC) can be effectively applied for longitudinal cohort evaluation of articular cartilage regeneration. Osteoarthritis and Cartilage. 2013;21(7):943-9.

32. Brama P, Tekoppele J, Bank R, Karssenberg D, Barneveld A, Weeren P. Topographical mapping of biochemical properties of articular cartilage in the equine fetlock joint. Equine veterinary journal. 2000;32(1):19-26.

33. Broster C, Burn C, Barr A, Whay H. The range and prevalence of pathological abnormalities associated with lameness in working horses from developing countries. Equine veterinary journal. 2009;41(5):474-81.

34. Eckstein F, Burstein D, Link TM. Quantitative MRI of cartilage and bone: degenerative changes in osteoarthritis. NMR in Biomedicine. 2006;19(7):822-54.

35. Murray RC, Branch MV, Tranquille C, Woods S. Validation of magnetic resonance imaging for measurement of equine articular cartilage and subchondral bone thickness. American journal of veterinary research. 2005;66(11):1999-2005.

36. Kidd J, Fuller C, Barr A. Osteoarthritis in the horse. Equine Veterinary Education. 2001;13(3):160-8.

37. Werpy NM, Ho CP, Pease A, Kawcak CE, editors. Preliminary study on detection of osteochondral defects in the fetlock joint using low and high field strength magnetic resonance imaging. Proceedings of the annual convention; 2008.

38. Eckstein F, Charles HC, Buck RJ, Kraus VB, Remmers AE, Hudelmaier M, et al. Accuracy and precision of quantitative assessment of cartilage morphology by magnetic resonance imaging at 3.0 T. Arthritis & Rheumatism. 2005;52(10):3132-6.

39. Cicuttini F, Morris KF, Glisson M, Wluka AE. Slice thickness in the assessment of medial and lateral tibial cartilage volume and accuracy for the measurement of change in a longitudinal study. The Journal of Rheumatology. 2004;31(12):2444-8.

3 Danksagung

An dieser Stelle möchte ich mich bei allen Personen ganz herzlich bedanken, welche mich fachlich und persönlich stets unterstützt haben.

Ganz besonders **meinen lieben Eltern**, welche mich in meinem beruflichen Werdegang grosszügig unterstützt haben,

Frau **Dr. med. vet. Andrea Bischofberger** für das interessante Thema und die jederzeit zur Verfügung stehende fachliche und motivierende Hilfestellung,

Herrn **Prof. Dr. med. vet. Anton Fürst** für die Übernahme des Referats,

Herrn **Prof. Dr. med. vet. Patrick Kircher** für die Unterstützung seitens der bildgebenden Diagnostik und der Übernahme des Korreferats,

Herrn **Prof. Dr. med. vet. Paul Torgerson**, für die Hilfe bei der statistischen Auswertung sowie

Frau **Dr. med. vet. Muriel Federici** und Frau **med. vet. Andrea Bachmann** für ihre Einsätze bei den Knorpelmessungen.

4 Curriculum Vitae

Name:	Regula Fürst
Geburtsdatum:	29.01.1977
Geburtsort:	Schlieren (ZH), Schweiz
Nationalität:	Schweiz
Heimatort:	Dietikon (ZH)

1984 – 1992	Grundschule und Sekundarschule Dietikon
1993 – 1997	Kantonsschule Urdorf (ZH)
1998 – 2003	Sekundarlehrerstudium phil. II an der Universität Zürich
2003 – 2007	Klassenlehrerin an der Oberstufe der Bezirksschule March in Lachen (SZ)
2007 – 2009	Cabin Crew Member bei Swiss International Airlines
2009 – 2014	Veterinärmedizinstudium an der Vetsuisse-Fakultät Zürich
2015 – 2016	Erstellen der Dissertation am Departement für Pferde unter der Leitung von Prof. Dr. med. vet. A. Fürst und der Betreuung von Dr. med. vet. A. Bischofberger, Vetsuisse-Fakultät der Universität Zürich

5 Anhänge

Table 5: Median and range of T1 and T2 relaxation times of the independent parameters in the generalized linear models. Thickness measurements divided in cartilage health and sagittal zones.
Abbreviations: mod. = moderate, n = number of samples

Independent parameters		**T1 (µm)**	**n**	**T2 (µm)**	**n**
Normal cartilage	condylar	1257 (590-1791)	27	1089 (569-1626)	27
	intercondylar	1050 (517-1632)	9	1145 (759-1944)	9
Mild – mod. cartilage disease	condylar	1180 (521-1748)	46	1061 (421-2177)	46
	intercondylar	1170 (516-1974)	17	1156 (468-1796)	17
Severe cartilage disease	condylar	975 (537-2030)	11	820 (311-1658)	11
	intercondylar	1085 (519-1592)	3	1441 (711-1559)	3

Table 6: Median and range of T1 and T2 relaxation times of the independent parameters in the generalized linear models. Thickness measurements divided in cartilage health and horizontal zones.

Abbreviations: mod. = moderate, n = number of samples

Independent parameters		**T1 (µm)**	**n**	**T2 (µm)**	**n**
Normal cartilage	dorsal	1050 (517-1791)	11	1061 (759-1411)	11
	central	1343 (590-1731)	16	1189 (569-1944)	16
	palmar	1142 (641-1490)	9	1089 (792-1283)	9
Mild – mod. cartilage disease	dorsal	917 (516-1458)	21	1078 (468-1670)	21
	central	1317 (717-1748)	25	1154 (421-2177)	25
	palmar	1126 (532-1974)	17	1127 (590-1796)	17
Severe cartilage disease	dorsal	1121 (1069-1191)	1	1138 (1083-1141)	1
	central	892 (519-2030)	8	930 (311-1658)	8
	palmar	1055 (537-1658)	5	813 (591-1516)	5

Table 7: Median and range of T1 and T2 relaxation times of the independent parameters in the generalized linear models. Thickness measurements divided in cartilage health and P2/P3.

Abbreviations: mod. = moderate, n = number of samples

Independent parameters		**T1 (µm)**	**n**	**T2 (µm)**	**n**
Normal cartilage	P2	1267 (590-1791)	22	1037 (569-1411)	22
	P3	1177 (517-1632)	14	1191 (759-1944)	14
Mild – mod. cartilage disease	P2	1099 (521-1748)	35	1084 (590-2177)	35
	P3	1263 (516-1974)	28	1134 (421-1965)	28
Severe cartilage disease	P2	975 (537-1658)	9	813 (311-1172)	9
	P3	1085 (519-2030)	5	1441 (711-1658)	5

Table 12: Median and range of TC, CC and HC of the independent parameters in the generalized linear models. Thickness measurements splitted in cartilage health and sagittal zones.
Abbreviations: mod. = moderate, n = number of samples, TC = total cartilage, HC = hyaline cartilage, CC = calzified cartilage

Independent parameters		**TC (µm)**	**n**	**HC (µm)**	**n**	**CC (µm)**	**n**
Normal cartilage	condylar	1827 (1068-3263)	27	1610 (1019-2961)	27	196 (84-351)	27
	intercondylar	2109 (1612-2561)	9	1992 (1462-2255)	9	241 (97-384)	9
Mild – mod. cartilage disease	condylar	1858 (1019-2838)	46	1674 (876-2654)	46	193 (77-406)	46
	intercondylar	2089 (999-3121)	17	1924 (767-3035)	17	183 (69-319)	17
Severe cartilage disease	condylar	1414 (885-1736)	11	1264 (695-1572)	11	204 (108-288)	11
	intercondylar	1829 (1285-2499)	3	1669 (1192-2237)	3	199 (124-267)	3

Table 13: Median and range of TC, CC and HC of the independent parameters in the generalized linear models. Thickness measurements splitted in cartilage health and horizontal zones.
Abbreviations: mod. = moderate, n = number of samples, TC = total cartilage, HC = hyaline cartilage, CC = calcified cartilage

Independent parameters		**TC (µm)**	**n**	**HC (µm)**	**n**	**CC (µm)**	**n**
Normal cartilage	dorsal	1886 (1500-2590)	11	1617 (1343-2272)	11	199 (123-384)	11
	central	2143 (1068-3165)	16	2020 (1456-2805)	16	209 (118-351)	16
	palmar	1480 (1186-3263)	9	1275 (1019-2961)	9	169 (84-352)	9
Mild – mod. cartilage disease	dorsal	1691 (1019-2554)	21	1527 (876-2307)	21	173 (69-406)	21
	central	2229 (1067-3004)	25	1987 (934-2807)	25	208 (77-331)	25
	palmar	1668 (999-3121)	17	1524 (767-3035)	17	197 (111-319)	17
Severe cartilage disease	dorsal	1450 (1429-1475)	1	1283 (1281-1293)	1	165 (154-197)	1
	central	1517 (885-2499)	8	1355 (787-2237)	8	171 (108-288)	8
	palmar	1288 (969-1892)	5	1054 (695-1686)	5	223 (147-273)	5

Table 14: Median and range of TC, CC and HC of the independent parameters in the generalized linear models. Thickness measurements splitted in cartilage health and P2/P3.
Abbreviations: mod. = moderate, n = number of samples, TC = total cartilage, HC = hyaline cartilage, CC = calzified cartilage

Independent parameters		**TC (µm)**	**n**	**HC (µm)**	**n**	**CC (µm)**	**n**
Normal cartilage	P2	1775 (1068-3263)	22	1570 (1019-2961)	22	197 (84-318)	22
	P3	2187 (1612-3165)	14	2052 (1462-2805)	14	214 (97-384)	14
Mild – mod. cartilage disease	P2	1759 (1019-2838)	35	1562 (876-2654)	35	191 (103-406)	35
	P3	2226 (999-3121)	28	1991 (767-3035)	28	194 (69-331)	28
Severe cartilage disease	P2	1358 (969-1736)	9	1228 (695-1504)	9	206 (136-288)	9
	P3	1574 (885-2499)	5	1375 (787-2237)	5	161 (108-267)	5